

Optimal synthesis, characterization, antibacterial and anticancer assay of green synthesized nickel nanoparticles by *Taxus brevifolia* leaf extract

S. Sarli¹, N. Ghasemi^{1*}, A. Moradi²

¹Department of Chemistry, Arak Branch, Islamic Azad University, Arak, Iran.

²Department of Microbiology, Faculty of Medicine, Golestan University of Medical Science, Gorgan-49177-65181, Golestan, Iran.

Submitted March 24, 2016; Accepted August 8, 2016

Nickel nanoparticles was synthesized by *T. brevifolia* leaves extract. This plant has promising medicinal properties for a wide range of cancer treatment. The goal was to conjugate *T. brevifolia* with Ni nanoparticles for enhanced anticancer effect. The effective parameters such as pH, volume of the extract, concentration of the salt solution, temperature and time were evaluated by Ultraviolet-Visible (UV-Vis) spectroscopy. According to the obtained results, reduction of nickel ions to nickel nanoparticles by *T. brevifolia* extract was optimum at pH=8, 2 ml of extract, 0.003M Ni(NO₃)₂, t=70 °C and time of 180 min. UV- visible, scanning electron microscope (SEM), field emission scanning electron microscope (FESEM), X-Ray Diffraction (XRD), FTIR spectroscopy and Transmission Electron Measurement (TEM) techniques were used to confirm the nanoparticles formation. Also, the antibacterial activity of *T. befolia* extract, nickel nanoparticles and nickel nitrate solution were tested. Their activity on *Staphylococcus-aureus*, *Escherichia-coli* and *Pseudomonas-aeruginosa* demonstrated that they don't have inhibitory effect on bacterial growth; and their anticancer activity were investigations by *Breast* cancer cell line *MCF-7*. The presence of taxol in the leaves of the *T. befolia* extract was confirmed by HPLC. Results demonstrated that in thick dilute solutions, nickel nanoparticles have more anti-cancer effects compared to the pure *T. befolia* extracts.

Keywords: T.befolia, Nickel nanoparticles, Antibacterial, Anticancer, Green synthesis, Characterization

INTRODUCTION

Metallic nanoparticles have attracted a great interest due to their optoelectronic and physicochemical properties. These properties depend on their size, shape, composition, and crystallinity. Recently, metallic nanoparticles synthesized by physical and chemical methods have attracted much interest due to their potential applications in various technological areas. Chemical action is the popular method for manufacture the metallic nanoparticles. However, some chemical methods cannot elude the utilization of toxic chemicals in the synthesis protocol; for example, hazardous substances such as *Tetrakis hydroxymethyl phosphonium chloride* (THPC)[1], *Poly-N-vinyl pyrrolidone* (PVP)[2] and hydroxylamine[3] are used for synthesis of metallic nanoparticles in traditional humid methods. Other dry methods such as UV-irradiation[4] aerosol[5] and lithography[6] are also not considered environmentally friendly. In the biological synthesis methods of nanoparticle using microorganisms[7], enzymes[8], and plant extracts[9] or plants[10] are possibly ecofriendly alternatives to chemical and physical methods, which is why focus has now shifted towards utilizing the biological action in the synthesis of metal nanoparticles.

Size and shape of NPs have a direct impact on the their physical and chemical properties. The physical and chemical properties of NPs are function of their size and shape. This difference in properties at nanoparticles are arising from to their large surface region which creates them very reactive and quantum size effects which become predominant at nanoparticles. Some the size dependent properties of NPs: Band Gap, the size of NPs decreases because the band gap between the conduction band and valence band is increases. Melting point, when the particle size gets below 5 nm, the phase transition temperature or the melting point of NPs is low and this decrease becomes more pronounced. Mechanical properties, at nanoscale, the probability of defects is low, just their mechanical strength is high and they are definition like hard materials and highly harsh. Electrical properties, the electrical conductivity is impress in 2 methods at nanoscale. It reduction because of big surface scattering while it may increase because of better arrangement. Optical properties, Dye or visual properties of NPs are very dependent on the size of particle. This change in color can be said on the basis of change of to higher wavelengths as the particle size large in case of plasmonic NPs. Magnetic properties, Ferromagnetism vanishes and shifts to supermagnetism applied to large surface energy of materials at nanoscale. Catalytic properties, the

* To whom all correspondence should be sent:
E-mail: n-ghasemi@iau-arak.ac.ir

catalytic application of NPs is development field as compared to bulk material just to their large surface field[11]. In the similar report the use of *Aegle marmelos* Correa leaf extract and *Coriander* leaf extract in the synthesis of nickel nanoparticles[12, 13]. The number of plants utilized in the biosynthesis keeps growing by the day as more researchers focus their attention to this new and relatively cheap and fast method of nanoparticle synthesis. Studies carried out on nickel nanoparticles synthesized using the physical methods are few [14] and even none for the biological method.

Nickel NPs find potential applications in various fields including electronics, magnetism[15], energy technology[16], and biomedicines[17]. Due to their high reactivity, operational simplicity, and eco-friendly properties they are used to catalyze various organic reactions including chemo-selective oxidative coupling of thiols, reduction of aldehydes and ketones[18], hydrogenation of olefins[19], synthesis of stilbenes from alcohol through Wittig-type olefination[20], and α -alkylation of methyl ketone[21]. They also catalyze certain inorganic reactions like decomposition of ammonia[22]. One of their recent applications is their role in the fabrication of carbon nanotubes (CNTs)[23]. Environmental applications of nickel nanoparticles were adsorption of hazardous dye and inorganic pollutants and thus play a vital role in the cleanliness of environment[24]. Due to their good antibacterial and anti-inflammatory activities they are used in the field of biomedicine[25]. They also show cytotoxicity against cancerous cells as is evident from the distortion of morphology of these cells after their treatment with Ni NPs[26]. The biocompatibility of Ni NPs capped with biomolecules such as glucose is highly increased and these are used as biosensors and heat nonmediator for cancer hyperthermia[27].

Taxol (paclitaxel) showed good effects as an anticancer agent[28, 29]. In the late 1950's, primary studies about the antimitotic property of *Taxol* started in connection with the National Cancer Institute (NCI) experimental program for cancer. *Taxol* was extracted for the first time from the stem bark of the yew tree (*Taxus brevifolia*) around the Pacific Ocean[30] and it has been isolated from many *Taxus* type, such as *T.brevifolia*, *T.cuspidata*, *T.baccata*, and *T.yunnanesis*. This substance is efficient against a variety of breast, skin and ovarian cancers because it prevents the depolymerization of tubulin[28, 29]. Chemical constituents of different *Taxus* species have been spaciouly studied for years, especially after *Taxol* recognition, a complex of diterpene alkaloid has been found in the bark of

Pacific yew tree. *T.brevifolia* has been conditioned as a noteworthy chemotherapeutic drug for breast and lung cancer treatment [30]. *Taxus* has attracted great attention due to its content of diterpene alkaloids, exclusively *Taxol* (also known as a generic drug paclitaxel and by the registered trade name *Taxol*(R) BMS [Bristol-Myers Squibb]). In 1970, the anticancer properties of *Taxol* were detected in *T.brevifolia* extracts[29].

In this report, *T.brevifolia* leaf extract used as reducing agent for reducing nickel ions presented in nickel nitrate solution. Synthesized nickel nanoparticles were evaluated by (UV-vis), (SEM), (FESEM), (XRD) and (FTIR) techniques. Antibacterial activity of *T.brevifolia* leaves extract, nickel nitrate solution and NiNPs were investigated on three bacteria contains *Staphylococcus-aureus*, *Escherichia-coli*, *Pseudomonas-aeruginosa*. As well as in this research, it has been attempted to increase the anticancer activity of nickel nanoparticles by synthesizing with *T.brevifolia* leavening extract. Anti-cancer activity of *T.brevifolia* leaves extract, nickel nitrate solution and NiNPs were investigated on *Breast cancer cell line MCF-7*. Transmission Electron Microscopy (TEM) was performed after determining the best dilution of nickel NPs solution for removing Breast cancer cells. TEM images demonstrate nickel NPs size.

MATERIALS AND METHODS

Materials

Leaves of *Taxus-brevifolia* were collected from southern mountains of *Ziarat* village at Gorgan, Iran (Figure 1). Nickel nitrate ($\text{Ni}(\text{NO}_3)_2$) were purchased from Sigma-Aldrich, and the other chemicals such as analytical grade sodium hydroxide and hydrochloric acid were purchased from Merck Darmstadt, Germany and deionized water was applicate throughout the experimental procedure in the laboratory. For HPLC test, the standard solution of *Taxol* (*Chemotaxel 30mg/5ml – Paclitaxel injection USP*) was purchased from the pharmacy at Gorgan.

For antibacterial activity test of nickel NPs, *Staph-ylococcus-aureus* (ATCC25923), *Escherichia-coli* (ATCC 1399) and *Pseudomonas aeruginosa* (ATCC 1430) were prepared from Iranian research organization of science and technology. *Breast cancer cell line MCF-7* was purchased from Pasteur Institute - Cell Bank, Iran.

Preparation of three extracts of *Taxus-brevifolia* leaves

Leafs, trunk, and shells of *T.brevifolia* tree were collected and washed thoroughly with double distilled water to remove dust. Then, they were dried separately and powdered and added some water to

them, till to be in the thick state and so the solution can spin on the shaker to have the most amount of *Taxol*. 20 grams of dried leaves, were boiled separately in 100 ml double distilled water at 40 °C, for 24hr. Extract was filtered through Whatman No.1 filter paper, centrifuged with the rate of 5000 rpm for 5 min and clear solution of the extracts were stored at 4 °C for further nanoparticles synthesis process.



Fig. 1. *T. brevifolia* tree and its leaves

HPLC test: Determine the best extract that contains the highest amount of Taxol

In order to find the amount of *Taxol* substance, leaves, trunk, and shells extracts of the *T.brevifolia* tree prepared and compared with the standard solution of *Taxol* (*Chemotaxel 30mg/5ml – Paclitaxel injection USP*). The extracts from leafs of *T.brevifolia* tree were analyzed for the presence of *Taxol* compounds by reverse phase HPLC Device (Agilent 1200). 2 μ L extract (100.0 μ g/mL) using C18 column (Agilent zorbox XDB-C18, 250 mm \times 4.6 mm) and UV detection was carried out at 227 nm according to the previous methods[31]. The mobile phase used in this study was acetonitrile: water (65:35, v/v) with 4.5 pH adjusted with acetic acid.

Synthesis of nickel nanoparticles using T. brevifolia extract

In order to find the best synthesis condition of nickel nanoparticles using *T.brevifolia* extract, the influence of pH, volume of extract, salt solution concentration, temperature and time have been studied. Change the color of the mixture indicated the formation of the nanoparticles and the aqueous metal ions reduced using plant extract (Figure 2). For this purpose, UV-Vis spectrophotometry has been used and each sample has been examined in the range of 200-580 nm. Metal-based nanoparticles have many free electrons that move by conduction and balance bands which is caused surface plasmon resonance (SPR) when the UV light collision to them. This spectrum records the vibrations of the free electrons nanoparticle. In this work a high peak which is appeared in the visible area also confirms the formation of metal nanoparticles.

Investigation of pH changing on the synthesis of nickel nanoparticles

0.5 ml of *T.brevifolia* extract and 0.001 M nickel nitrate solution were added into 7 vials. The pH of each vial was adjusted to 2,4,5,6,7,8,9 by 0.1 M NaOH and 0.1 HCl and stirred with the stirring rate of 150 rpm for 30 min at room temperature. By adding metallic salt solution, the color of *T. brevifolia* extract solution obviously changed from light yellow to orang which was indicated the formation of nickel nanoparticles. After a while these solutions were centrifuged with stirring rate of 5000 rpm for 30 min, then solution was separated from the sediment and UV spectrum was recorded and the best pH for this synthesis has been determined. pH was adjusted to this value for further experiments. (Figure 3)

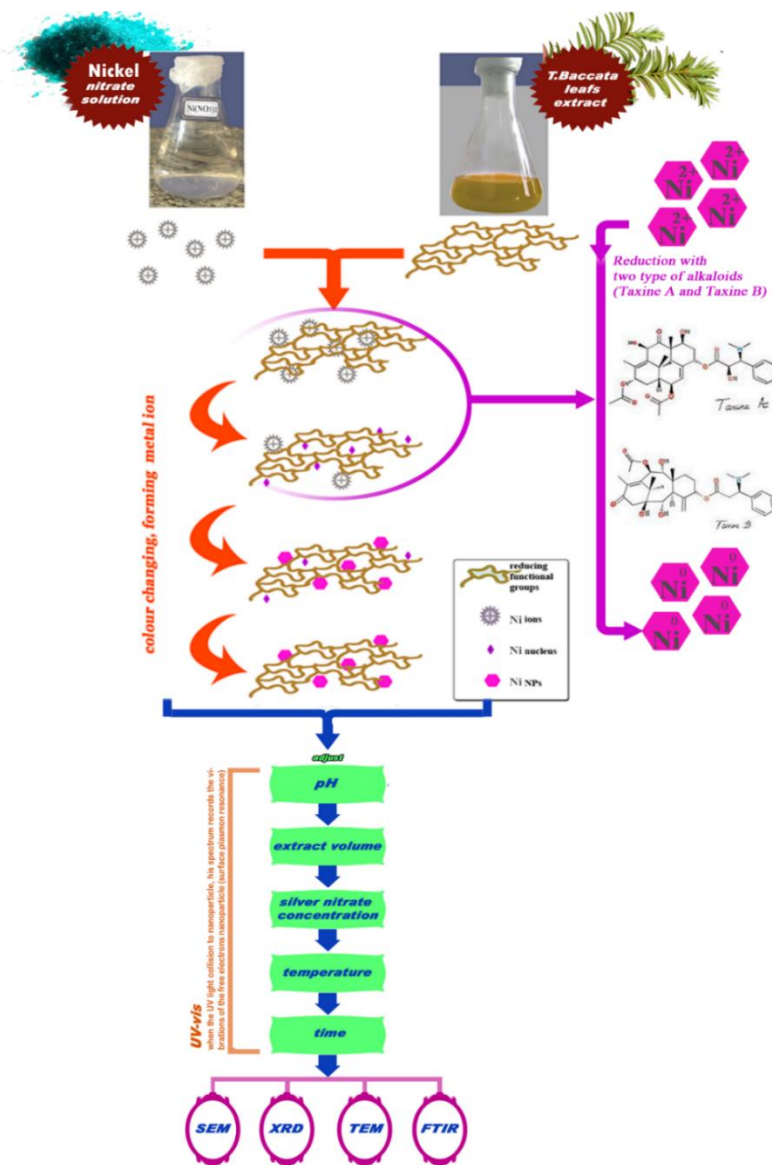


Fig. 2. A mechanism of nickel nanoparticle synthesis using by *T.brevifolia* extract

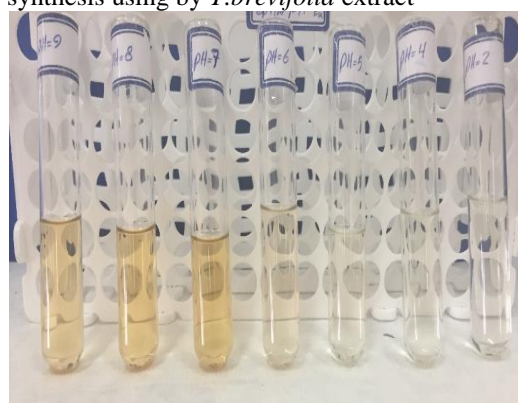
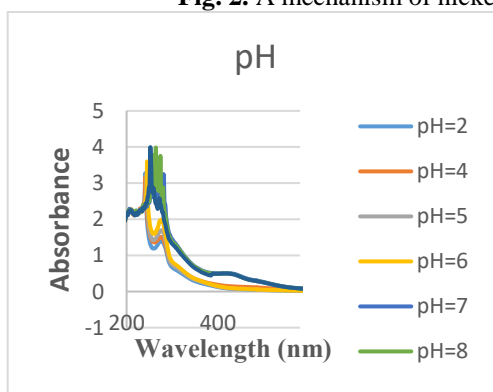


Fig. 3. Effect of pH on nickel nanoparticles synthesis by *T.brevifolia* extract (0.5 ml of extract solution, 5 ml of 0.001 M nickel nitrate, time: 30 min, stirring rate 150 rpm)

Investigation of extract volume changes on nickel nanoparticle synthesis

5 ml of 0.001 M nickel nitrate was poured into 6 vials and 0.2, 0.25, 0.5, 1, 1.5 and 2ml of *T.brevifolia* extract solution was added to them. Then the pH of all vials were adjusted to the optimized pH and

stirred with the stirring rate of 150 rpm for 30 min at room temperature, after that solutions were centrifuged and separated from the sediment and UV spectrums were recorded like the past step. Thus the best volume has been determined and used for further experiments. (Figure 4)

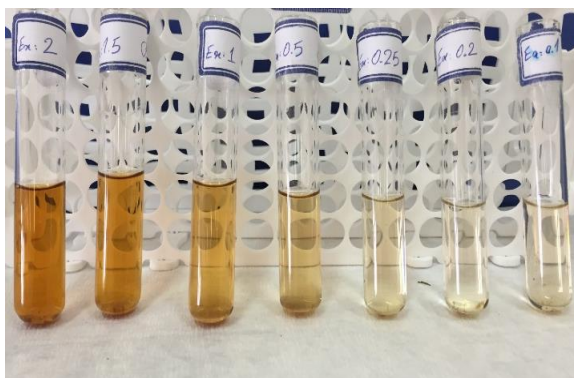
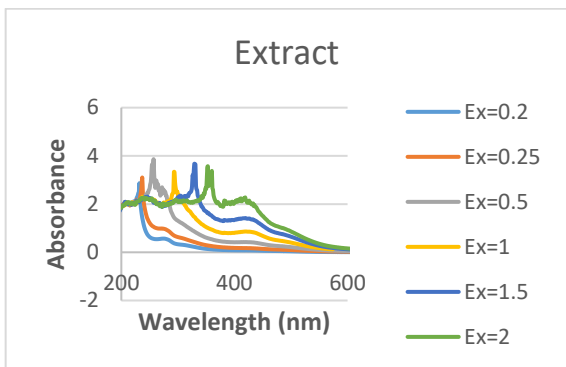


Fig. 4. Effect of *T.brevifolia* extract solution on nickel nanoparticles synthesis (pH of the solution was 8, 5 ml of 0.001 M nickel nitrate, time: 30 min, stirring rate 150 rpm)

Investigation of nickel nitrate molar changing on nickel nanoparticle synthesis

In order to optimize the concentration of metallic salt solution, 2 ml of *T.brevifolia* extract was poured into 6 vials then 5 ml of 0.0005, 0.001, 0.0015, 0.002, 0.0025, and 0.003 M nickel nitrate was added to them. the pH of all vials were adjusted to

optimized pH and after a while these solutions stirred with the stirring rate of 150 rpm for 30 min then the solution was separated from the sediment and UV spectrum was recorded. Therefore, the concentration was optimized and used for next experiments (Figure 5).

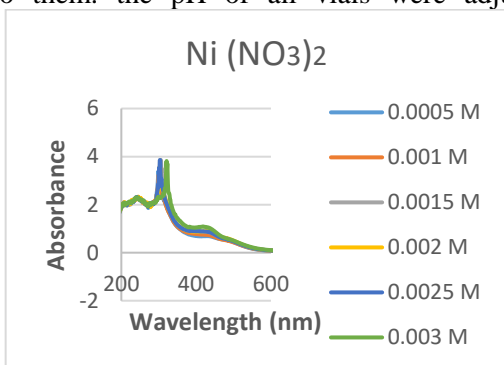


Fig. 5. Effect of nickel nitrate solution concentration on nickel nanoparticles synthesis by *T.brevifolia* extract (pH of the solution was 8, 2 ml of the *T.brevifolia* extract, time: 30 min, stirring rate 150 rpm)

Investigation of temperature changing on nickel nanoparticle synthesis

By following the previous optimum parameters, the optimal temperature was investigated. 2 ml of *T.brevifolia* leaves extract and 5 ml of nickel nitrate 0.003 M were poured into 8 vials and pH was set at

8. Then all vials were heated at 25, 35, 40, 50, 60, 70, 80 and 90°C for 1 hour. After that all samples were centrifuged and UV spectrum were recorded with the same conditions as before. So the optimal temperature was obtained (Figure 6).

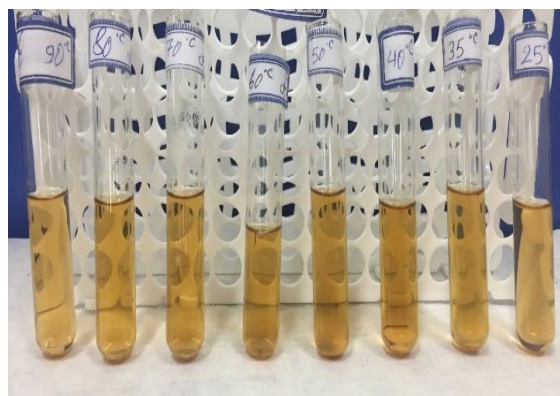
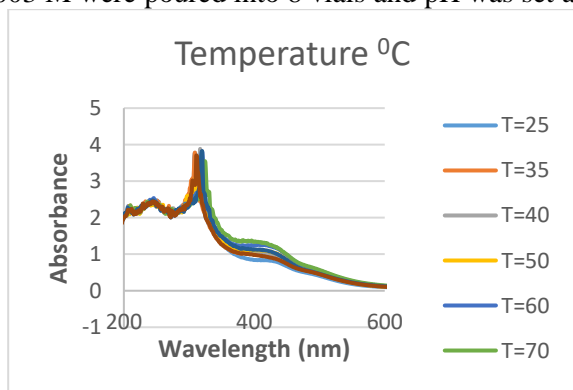


Fig. 6. Effect of temperature on nickel nanoparticles synthesis by *T.brevifolia* extract (pH of the solution was 8, 2 ml of the *T.brevifolia* extract, 0.003 M nickel nitrate, time: 30 min, stirring rate 150 rpm)

Investigating the effect of time on nickel nanoparticles formation

Specify the appropriate time for metallic nanoparticles synthesis is an important step because metallic ions increase and release at the specific time, then the surface plasmon resonance decreased. 2 ml of *T.brevifolia* extract and 5 ml of nickel nitrate

(0.003 M) were poured into 12 vials and the pH was set on 8 and heated to 70°C then centrifuged and UV spectrum were recorded after 5, 10, 15, 20, 30, 40, 60, 90, 120, 150, 180, 210 min respectively. According to the results, the best time for nanoparticle synthesis was determined (Figure 7

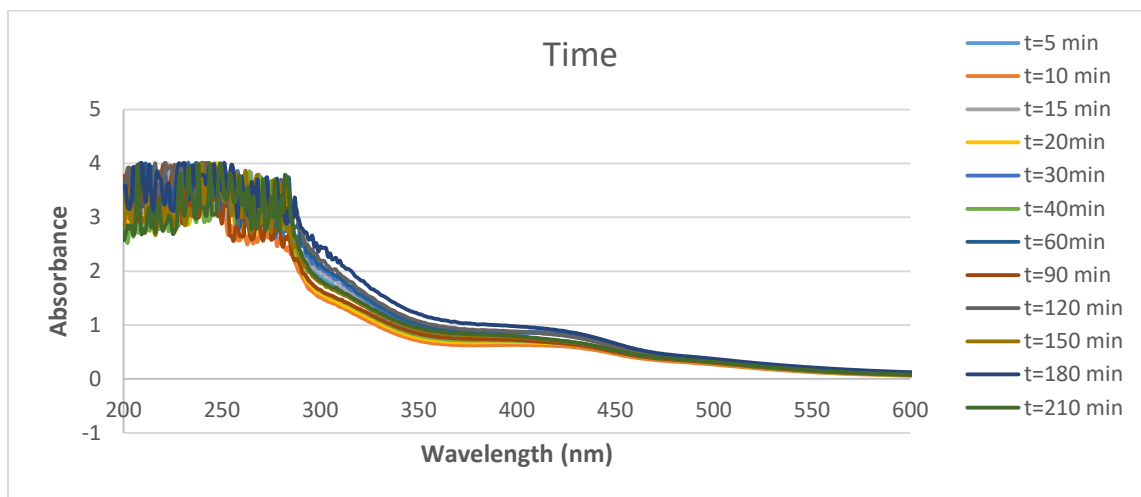


Fig. 7. Effect of time on nickel nanoparticles synthesis by *T.brevifolia* Extract (pH of the solution was 8, 2 ml of the *T.brevifolia* extract, 0.003 M nickel nitrate, temperature 70°C, stirring rate 150 rpm)

Characterization of the green synthesized nickel nanoparticles using *T.brevifolia* leaves extract

According to the previous experiments and obtained results from the UV spectra for the studied parameters (Figure 3 to Figure 7) the optimal parameters which are affecting nickel nanoparticles synthesis using *T.brevifolia* extract were determined. According to the UV spectra results for the studied optimal parameters, nickel nanoparticles were synthesized again. So 20 ml of *T.brevifolia* extract was added to 50 ml of 0.003 M nickel nitrate solution, pH was set on 8 and placed into the incubator at 70 °C for 180 min, it was centrifuged for 5 minutes, the obtained nickel nanoparticles were characterized by using different techniques such as UV, SEM, FESEM, XRD, TEM and FTIR. For nickel NPs, *T.brevifolia* extract and nickel nitrate solution, antibacterial activity by well test and MIC, as well as anticancer activity by MTT method were studied.

Determination of antibacterial activity

Nickel nanoparticles synthesized using *T.brevifolia* extract were tested for antimicrobial activity by agar diffusion method against different three bacterizes, such as *Staph-ylococcus-aureus* (ATCC25923), *Escherichia-coli* (ATCC 1399) and *Pseudomonas-aeruginosa* (ATCC 1430)

prepared from Iranian research organization for science and technology. The pure cultures of bacteria were subculture on nutrient agar. Each Bacteria with concentration of 0.5 McFarland was swabbed uniformly onto the individual plate using sterile cotton swabs. Using gel puncture method, 10 Wells of 6 mm diameter were made on nutrient agar plates.

Considered plats with separate bacteria for comparison the antibacterial effects of *T.brevifolia* extract, nickel nitrate solution, and nickel nanoparticles. Nickel nitrate solution and nickel nanoparticles solution were diluted individually.

100 mM nickel nitrate solution was prepared and diluted 7 times by deionized water: (1/1): 50 mM, (1/2): 25 mM, (1/4): 12.5 mM, (1/8): 6.25 mM, (1/16): 3.1 mM, (1/32): 1.5 mM and (1/64): 0.75 mM. Several sets of three selected bacterial culture plates were provided for investigation of the antibacterial effects of three case study solutions including *T.brevifolia* extract, nickel nitrate solution, and nickel nanoparticles solution. Equal volumes of 100 µl of each dilution applied to a set of three selected bacterial culture as described above. Same sets of three bacterial culture plates were considered without any additive material as well as with cephalixin standard antibiogram disks as the negative and positive controls respectively. All plates were evaluated after a 24 hours incubation

period at 37°C. The inhibition zone of the bacteria was accurately measured by the caliper and the mean diameter of the bacterial inhibition zone and the comparison with positive and negative control were considered as an indicator of antibacterial activity evaluation. Each assay was repeated for three times as described previously [32, 33].

Minimum inhibitory concentration (MIC) Test

The minimum concentration of growth inhibitory was determined for aqueous *T.brevifolia* extract, nickel nitrate solution and nickel nanoparticle synthesized using *T.brevifolia* extract. Like the previous step, serial dilutions of nickel nitrate solution and nickel nanoparticle were prepared. Using a 96-well plate, a set of 7 wells were considered separately for each study materials containing 100 µl of the serial diluents. Then, 100 µl of brain-heart-infusion-broth (BHI) solution and 100 µl of active bacterial suspension 1.5×10^6 cfu/ml were added to each well. The Same procedure was performed for all three bacterial species. for each run of the experiments positive and negative controls were considered as well. Positive control wells included the relevant bacteria with BHI solution and negative control included the case study solution (extract, silver nitrate or silver nanoparticles) with BHI solution. Finally, the plate was incubated for 24 hours at 37°C. After incubation, the turbidity of the wells, which was due to the growth of the bacteria, was investigated and called OD. The first dilution with no turbidity (lack of growth) was recorded as the minimum deterrent concentration [34,35]. To reduce the experimental errors, all experiments were repeated four times.

Investigation the anticancer activity by MTT assay

According to the previous step, 7 dilutions of case study solutions were prepared for MTT test. The human Breast cancer cell line MCF-7 cells were cultured in Dulbecco's Modified Eagle's Medium (DMEM), supplemented with 10% fetal bovine serum at 37°C with 5% CO₂. Cells were placed in 96-well plates (8.10^3 cells/well) containing 100 µL of medium. After 24 h, different concentration of nickel nanoparticles, extract and nickel nitrate solution were dispersed in DMEM medium, after that they were added to each well and incubated for 24 h. Growth of the cells was quantified by the ability of living cells to reduce Pink dye MTT to a pale violet formazan product. After 24 h incubation fresh medium (100 µL) containing 0.5 mg/mL of MTT was replaced by the previous in each well. After 4 hours, the formazan product of MTT reduction was dissolved in DMSO and the absorbance was

measured using a microplate reader. Effect of nickel nanoparticles as the percentage of control absorbance of reduced dye was measured at 570 nm.

RESULTS AND DISCUSSION

High-performance liquid chromatography (HPLC) experiment for determining Taxol in the extracts

HPLC experiment was applied for determining Taxol in the extracts. The standard solution of Taxol showed an absorption of 350 mAU at 24-25 minutes after injection (Figure 9-a). No pick was observed after injection of the extracts of the crust (Figure 9-b) and the stem (Figure 9-c) at this time. However, a significant pick of 350 mAU absorption was observed at 24-25 minutes after injection of the leaf extract of yew tree (Figure 9-d, e). Therefore, the leaf extract only which was confirmed to have the proper amount of Taxol was applied for the rest of the present study.

Ultraviolet-visible spectroscopy (UV-Vis):

UV-Vis spectra shows the effect of different optimal parameters which is affected nickel nanoparticles synthesis using *T.brevifolia* extract. Metal nanoparticles have many free electrons that move by conduction and balance bands which is caused surface plasmon resonance (SPR) when the UV light collision to them, this spectrum records the vibrations of the free electrons nanoparticle. In aqueous solution, nickel nitrate dissociates into negative nitrate anions and positive Ni²⁺ cations as given in Figure 2. The hydrated electrons of *T.brevifolia* leaf extract aqueous reduce Ni²⁺ cations into zero valent nickel (Ni⁰) by nucleation process. Many Ni⁰ atoms agglomerate to form Ni_n⁰. This phenomenon of agglomeration is due to the binding energy between two metal atoms which is stronger than the atom-solvent bond energy as previously reported for Ni₂⁰ by Huimei & et al [36] and for Ag⁰ by Kazem & et al [37]. Since nickel atoms attract each other by dispersion while encountering progressively coalesce into the growing clusters by a cascade of coalescence processes, which is in a good concurrence with earlier reports [34,37]. In this work, a high peak which was appeared in the visible area also confirmed nickel nanoparticles formation and SPR absorption band in the final investigation was observed around at 270 nm wavelength region due to the presence of orange-colored nickel nanoparticles synthesized. Similar results were reported by Solomon et al [38].

SEM and FESEM analysis

Surface morphology of the as formed nickel NPs was studied applying SEM. SEM analysis displayed

the presence of nanoparticles accumulation. SEM images (Figure 10) of Ni nanoparticle which was synthesized using *T.brevifolia* extract were tested using VEGA-TESCAN SEM analyzer with

acceleration voltage of 15kV and 1,04 μ m resolution. It was observed in the images that the small size of the nickel nanoparticles was 52 nm.

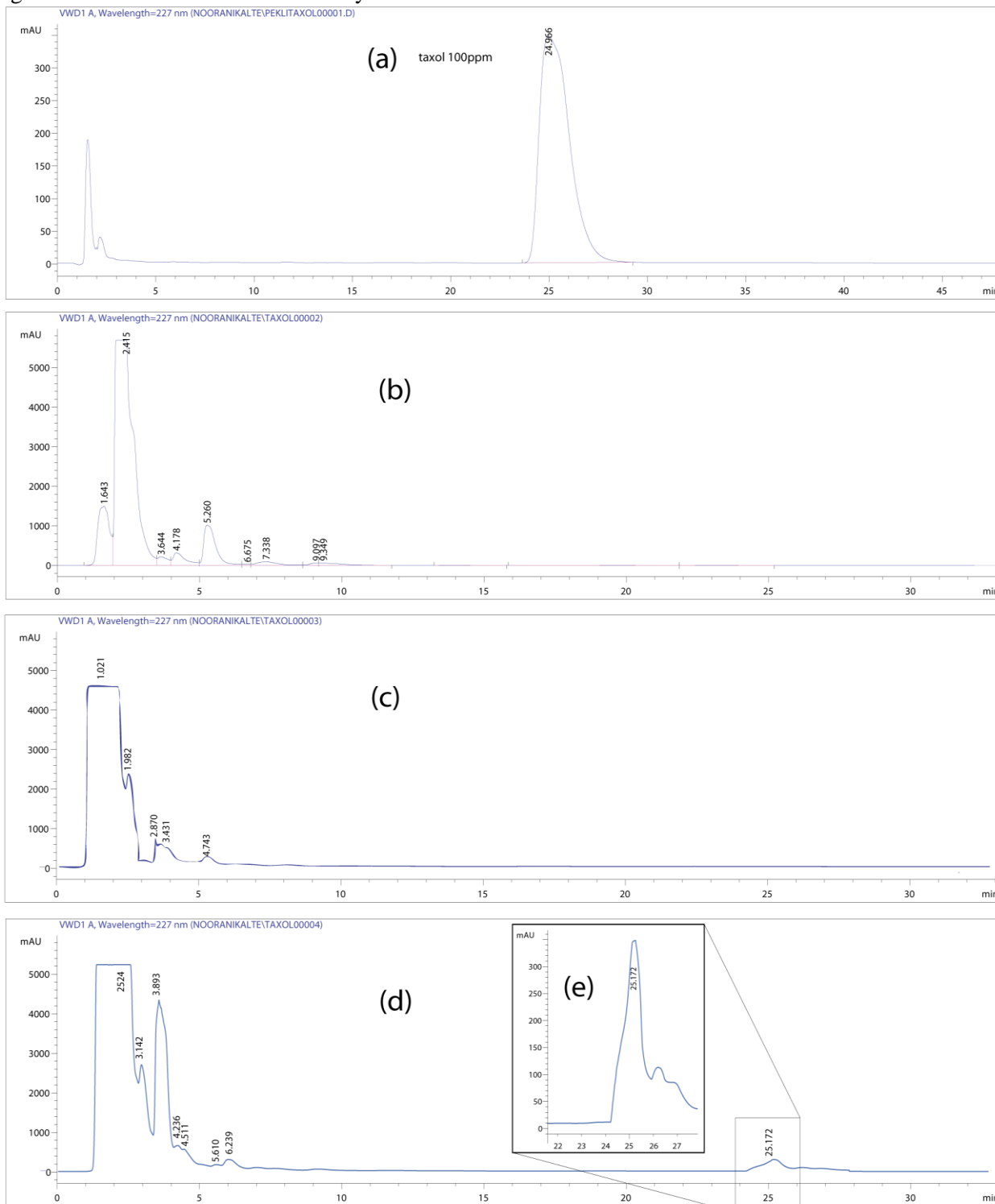


Fig. 9. The standard solution of Taxol (a). The extracts of the crust (b). The extracts of the stem (c). The leaf extract of yew tree (d, e).

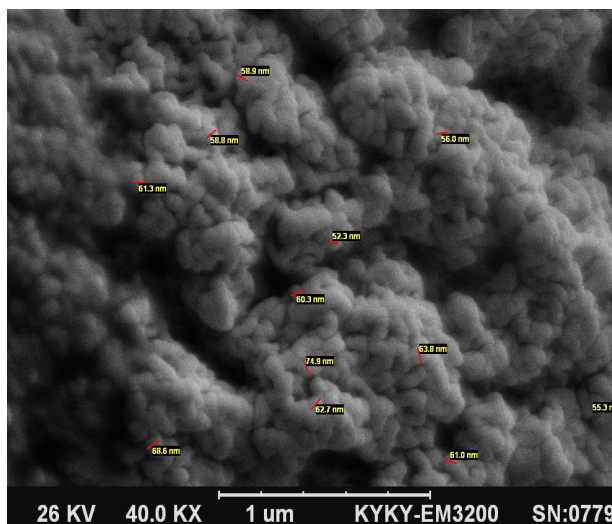


Fig. 10. SEM images of nickel nanoparticles synthesized by *T.brevifolia* extract.

The morphologies of the nickel nanoparticle which was synthesized using *T.brevifolia* extract were examined using MIRA3TESCAN-XMU FESEM analyzer (Figure 11) with acceleration voltage of 15kV and 0.692 μm resolution. It was observed in the images that the average size of the nickel nanoparticles was 22 nm. Pandian & et al[39] with *Ocimum sanctum* leaf extract and Angajala & et al[40] with aqueous leaf extracts of *Aegle marmelos Correa* synthesized nickel nanoparticle and reported SEM image of their nanoparticles.

X-Ray Diffraction (XRD) Analysis

Particle size of the sample were investigated using X-ray diffraction (XRD) technique. X-ray diffraction (XRD) analyses were carried out with a GNR MPD 3000 made Italy diffractometer using a

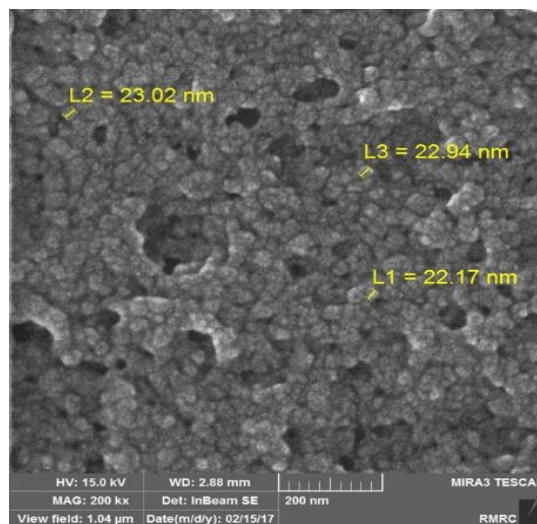


Fig. 11. FESEM images of nickel nanoparticles synthesized by *T.brevifolia* extract

Cu anode ($\lambda = 1.54056 \text{ \AA}$). The diffractograms were recorded at 2θ in the range $4^\circ - 90^\circ$, counting time is 0.5 second and with step size of 0.02° . Crystallite size is calculated using Scherrer equation[41]:

$$D = \frac{0.89 \lambda}{\beta \cos\theta}$$

Where, D- is the crystallite diameter size (nm), λ - X-ray wavelength, β - is full width at half-maximum (FWHM) and θ is Bragg's angle of reflection. According to the X-ray diffraction pattern of synthesized nickel nanoparticles using *T.befolia* extract three highest peaks at about $2\theta = 33.86^\circ$ (128), 29.43° (375) and 23.62° (330) planes, respectively, which are characteristic of the hexagonal structure of Ni-NPs (Table 1).

Table 1. XRD peak List data of NiNPs synthesis using *T. brevifolia* extract

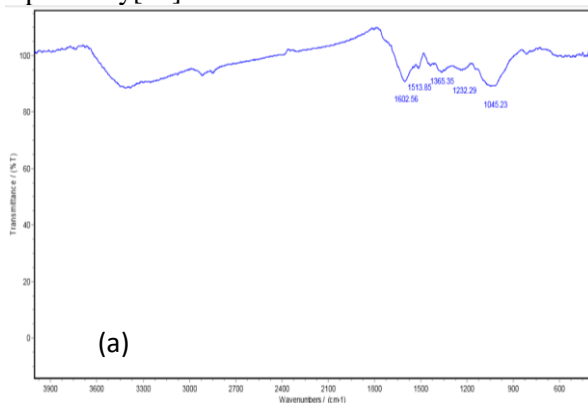
Pos. [2θ .]	Height [cts]	FWHMLeft [2θ .]	d-spacing [\AA]	Rel. Int. [%]
19.32	73	0.32	4.59093	19.57
23.629	330	0.20	3.76223	88.01
27.36	136	0.13	3.25730	36.18
28.37	34	0.3	3.14341	9.12
29.432	375	0.15	3.03233	100.00
32.42	87	0.1	2.75973	23.09
33.86	128	0.41	2.64510	34.07
41.18	67	0.2	2.19013	17.82
46.67	55	0.29	1.94458	14.56
68.142020	15.824230	0.358176	1.37613	4.22

According to Govindasamy & et al[42] researches the surface morphology of nickel nanoparticles was irregular polygonal, cylindrical and spherical in shapes. In this work, the size of nickel nanoparticle from the three highest peaks of the (FWHM), was calculated using *Scherrer-Debye* equation which was 53 nm (Figure 12). The results of the X-Ray analysis indicated that hexagonal nickel nanoparticles were formed by Ni²⁺ using *T. brevifolia* leaves extract.

To elucidate the nature of phytochemicals responsible for nickel nanoparticles reduction (Figure 13-a) and *T. brevifolia* extract (Figure 13-b), FTIR spectrometry was studied (Rayleigh WQF-510A spectrometer). This study was performed to recognize the various functional groups for capping and efficient stabilizing of the synthesized nickel nanoparticles. To elucidate the nature of phytochemicals responsible for nickel nanoparticles reduction (Figure 13-a) and *T. brevifolia* extract (Figure 13-b), FTIR spectrometry was studied (Rayleigh WQF-510A spectrometer). This study was performed to recognize the various functional groups for capping and efficient stabilizing of the synthesized nickel nanoparticles.

FT-IR studies

Spectra for characterizing dried powders were recorded in the range of 4000–400 cm⁻¹ using KBr pellet method. Based on FTIR results the observed bands at 3418 and 2920 cm⁻¹ can be assigned to the –OH and aldehyde C–H stretching vibrations, respectively[43]. The band located at 2355 cm⁻¹ is



attributed to the N–H stretching/C55O stretching vibrations[44]. The band at 1635 cm⁻¹ corresponds to amide I, which arises due to carbonyl stretching vibrations in proteins[45].

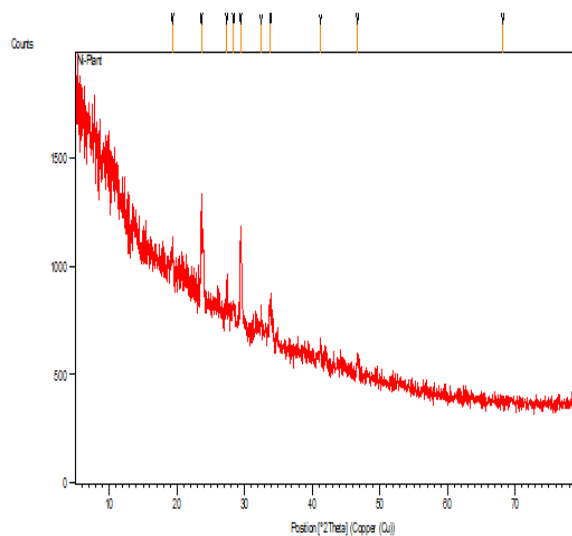


Fig. 12. X-ray diffractogram of nickel nanoparticles synthesized by *T. brevifolia* extract.

The characteristic bands observed at 1380 and 1079 cm⁻¹ are attributed to the C55O and C–O stretching vibrations, respectively[43,44,45]. Based on the analysis it is clear that the alkaloids may be adsorbed on the surface of nickel nanoparticles by a possible interaction via carbonyl groups or π -electrons. The peak intensity has been trimmed when Ni²⁺ is reduced to Ni⁰ for the formation of Ni NPs[46] which is showed in Figure 2.

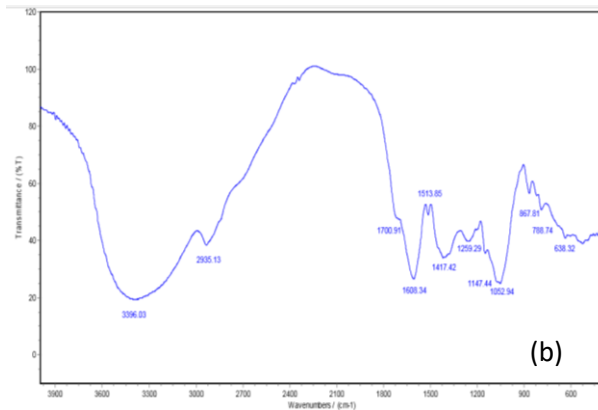


Fig. 13. FT-IR spectra of (a) *T. brevifolia* extract (b) nickel nanoparticles synthesized by *T. brevifolia* extract

The presence of biomass over the surface of nickel nanoparticles may cause steric or electrostatic barriers, which effectively prevented the accumulation of nanoparticles. Mallikarjuna & et al[47] reported that the carbonyl and hydroxyl groups from amino acid residues or proteins can strongly bind to metal nanoparticles like capping agent and stabilize the nano-particles by preventing their agglomeration. It can be observed that nickel

nanoparticles were successfully synthesized using *Taxin A* and *Taxine B* in the *T. brevifolia* extract. Evanoff & et al[48] suggested that the biological molecules exhibit dual role of formation and stabilization of nanoparticles in the aqueous medium. Finally, the synthesis of nickel nanoparticles using different plants is compared with our study in the Table 2

Table 2. recent research of nickel nanoparticles synthesized from plant extracts

Authors	Plant	Biological agent involved	Optimized condition	Size (nm)	Max peaks in SPR (nm)	shape	Analytical Methods	References year/
Solomon A. Mamuru, Nurudeen Jaji	<i>Moringa oleifera</i> leaf extract	amino aryl ketones associated with anthraquinones	- one step	-	297	-	UV-Vis, FTIR, AFM, EIS	2016 [38]
Chitra Jeyaraj Pandian¹ and et al	<i>Ocimum sanctum</i> leaf extract	biological molecules	- one step	30	395	polygonal, cylindrical and spherical	UV-Vis, FTIR, XRD, SEM, TEM	2015 [39]
Angajala, G. and et al	aqueous leaf extracts of <i>Aegle marmelos</i> Correa	Hydroxyl groups	- one step	80-100	250-400	face centered cubic	UV-Vis, FTIR, XRD, SEM, AFM and TGA	2014 [49]
Vasudeo K¹ and Pramod K	Leaf Extract of Coriander	phenolic compounds	- one step	30.71	560	face centered cubic	UV-Vis, FTIR and XRD	2016 [50]
Chitra Jeyaraj Pandian and et al	<i>Ocimum sanctum</i> Leaf Extract	amino acid residues or proteins in the extract	- one step	12 and 36	-	spherical	FTIR and TEM	2016 [51]
Ganesh Elango and et al	Methanolic extract of <i>Cocos nucifera</i>	C=O	- one step	47	252	cubical	UV-Vis, FT-IR, XRD, SEM, DAX, TEM	2016 [53]
Palanivel Rameshthangam, Jeyaraj Pandian Chitra	<i>Ocimum sanctum</i> leaf extract	Carboxyl with the catechol group	- one step	40 to 65	404, 257-416	face-centered-cubic	UV-vis, FTIR, XRD, SEM,	2017 [54]
Solomon A. Mamuru	<i>Annona Squamosa</i> Leaf Extract	aromatic amine	- one step	-	285	-	UV-Vis, FTIR,	2015 [52]
Sarli S et al	<i>T. befolia</i> leaf extract	Alkaloids: Taxan A and Taxan B	adjusted of pH, volume of extract, nickel nitrate concentration, temperature and time	SEM =52 TEM =50 XRD =53	270	Hexagonal	UV-Vis, SEM, FESEM, FTIR, XRD, TEM	This report

Antibacterial effect of nanoparticle against tree bacteria

Serial dilutions of nickel NPs solution and nickel nitrate solution did not show antimicrobial effects on *staph*, a germ-positive bacteria, and on the gram-negative bacteria like *E.coli* and *pseudomonas*. As well as pure *T.brevifolia* extract did not show the inhibition zone in the wells. MIC Test for pure *T.brevifolia* extract, nickel nitrate solution and nickel nanoparticle to inhibit growth were

determined. Results show no antibacterial activity for the pure *T.brevifolia* extract, but while nickel nanoparticle synthesized using *T.brevifolia* extract and nickel nitrate solution have more antibacterial activity (Table 3). Both nickel nitrate solution and nickel nanoparticles have higher suppressive effects on *P. aeruginosa* and *Staph. aureus* bacteria comparing the *E. coli* bacteria.

Table 3. MIC of *T.brevifolia* extract, nickel nitrate and nickel NPs

Organism	Sample	MIC (mM)
Staph. aureus	nickel nanoparticle synthesized by <i>T. befolia</i> extract	12.5 mM (74mg Ni(NO ₃) ₂ / 10ml)
	nickel nitrate	12.5 mM (74mg Ni(NO ₃) ₂ / 10ml)
	<i>T. befolia</i> extract	0.0 (2g/10ml)
E. coli	nickel nanoparticle by synthesized by <i>T. befolia</i> extract	25 mM (148mg Ni (NO ₃) ₂ / 10ml)
	nickel nitrate	25 mM (148mg Ni (NO ₃) ₂ / 10ml)
	<i>T. befolia</i> extract	0.0 (2g/10ml)
P. aeruginosa	nickel nanoparticle by synthesized by <i>T. befolia</i> extract	12.5 mM (74mg Ni (NO ₃) ₂ / 10ml)
	nickel nitrate	12.5 mM (74mg Ni (NO ₃) ₂ / 10ml)
	<i>T. befolia</i> extract	0.0 (2g/10ml)

Assessment of anticancer activity by MTT assay

Anti-cancer activity of nickel nanoparticles synthesized using *T.brevifolia* extract at various concentrations was investigated. Synthesized nickel nanoparticles have more anticancer activity compared to the pure *T.brevifolia* extracts. Their anticancer activity tends to be more effective in more concentrated solutions. In 6.2 mM nickel nanoparticle, about 78% the cancer cells were dead. Extract in the half dilution state showed the most

anti-cancer activity and about 72% of cancer cells die. 50 mM nickel nitrate solution exhibited about 90% inhibition of cancer cells growth and in the most soluble state showed the lowest anti-cancer activity and suitable anticancer activity (Figure 14). Breast cell proliferation inhibitory activity of the *T.brevifolia* extract, nickel nitrate, and NiNPs synthesized with *T.brevifolia* leaves extract are given in Table 4.

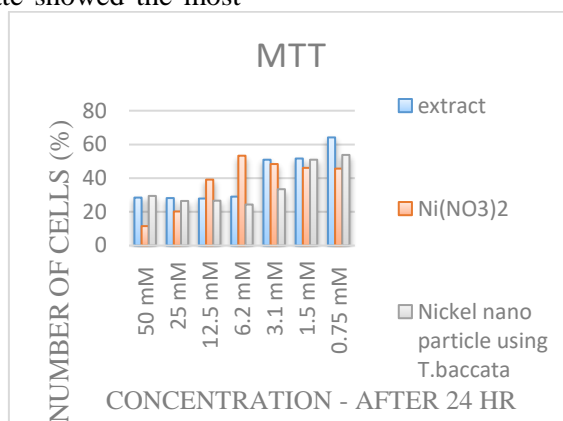


Fig. 14. MTT assay for the nickel nanoparticles, extract containing Taxol and nickel nitrate solution using the *Breast* cell line.

Transmission electron microscopic (TEM)

Transmission electron microscopic (TEM) image of synthesized nickel nanoparticles reveals the shape and size of nickel nanoparticles. TEM measurements were performed on Zeiss model EM900 instrument operated at 80 kV accelerating voltage. Among the as-prepared nickel nanoparticle solutions, we chose

a dilution that showed the best anti-cancer activity to kill the cancer cells. For TEM measurements by placing a drop over carbon coated copper grids and allowing the solvent to evaporate. TEM imaged are presented in Figure 15. The TEM micrograph suggests that the size of particles is about 50 nm. However, nanoparticles size in SEM and XRD were

about 52 and 53 nm, respectively. The agglomeration property of the nanoparticles is due to magnetic interaction and polymer adherence between the particles as reported earlier by Wang & et al [55].

CONCLUSION

Nickel nanoparticle synthesized by *T. brevifolia* leaves extract and important parameters were investigated. Synthesis of NiNPs using *T. brevifolia* showed good results for biomedical applications. An absorption peak at 270 nm in UV–vis spectrum have been proven the formation of NiNP using *T. brevifolia*. The obtained results from Vis-UV spectrophotometry, as well as SEM, XRD and FTIR, confirmed the efficiency of *T. brevifolia* leaves extract in the synthesis hexagonal nickel nanoparticles. In FTIR spectrum of the NiNPs and extract, reducing functional groups for nickel ions reduction were observed. Therefore, it can be concluded that synthesis of metallic nanoparticles using herbal extracts instead of chemical and physical methods

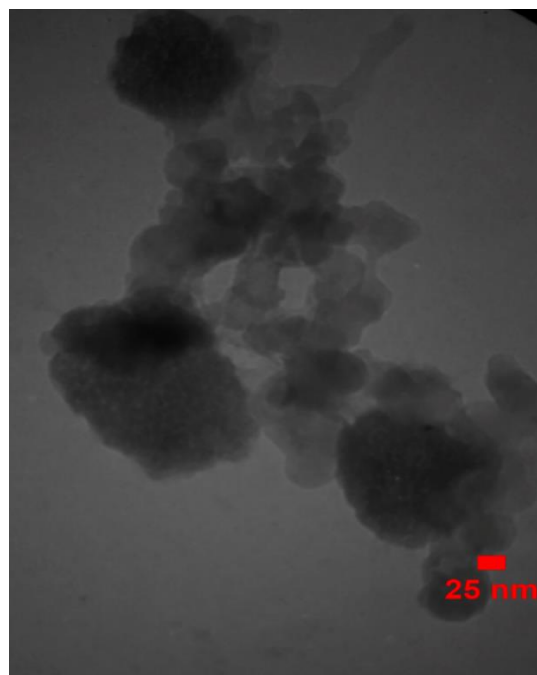


Fig. 15. Transmission electron microscope (TEM) of nickel nanoparticles synthesized by *T. brevifolia* extract.

Table 4. Breast cell proliferation inhibitory activity of *T. brevifolia* extract, nickel nitrate and nickel NPs

The solutions studied	No.	Concentration of nickel nitrate (mM)	Dilutions	% Cell viability (±1)	% Cell inhibition (±1)
NiNPs synthesized by <i>T. brevifolia</i> extract	1	0.75	1/64	53.77	46.23
	2	1.5	1/32	50.92	49.08
	3	3.1	1/16	33.42	66.58
	4	6.25	1/8	24.32	75.68
	5	12.5	1/4	28.6	71.4
	6	25	1/2	28.45	71.55
	7	50	1/1	31.43	68.57
Ni nitrate	1	0.75	1/64	45.64	54.36
	2	1.5	1/32	46.08	53.92
	3	3.1	1/16	48.36	51.64
	4	6.25	1/8	63.3	36.7
	5	12.5	1/4	39.11	60.89
	6	25	1/2	20.2	79.8
	7	50	1/1	11.52	88.48
<i>T. brevifolia</i> extract	1	0	1/64	64.15	35.85
	2	0	1/32	51.63	48.37
	3	0	1/16	49.92	50.08
	4	0	1/8	29.01	70.99
	5	0	1/4	27.88	72.12
	6	0	1/2	28.16	71.84
	7	0	1/1	28.45	71.55

for preparation of these nanoparticles is an appropriate alternative. The obtained results from high throughput techniques like UV-visible spectroscopy, FTIR, SEM and XRD measurements indicated the successful formation of NiNPs.

Antibacterial activity of different dilutions of *T.brevifolia* extract, nickel nanoparticles and nickel nitrate solution were studied. Inhibition area did not observed around the wells in the *E.coli*, *Staphylococcus aureus* and *P.aeruginosa* plates. The extract did not show any antibacterial effect. It was found that the presence of Taxol, which is a toxic substance, in the extract has not affected the growth of bacteria. MIC test of Nickel nitrate solution and Ni nanoparticle showed similar results. This means that the addition of *T.brevifolia* extract did not have much effect on the release antibacterial activity of nickel nanoparticles. Average MICs were concluded and 12.5 mM for *Pseudomonas* and *Staphylococcus-aureus*, 25 mM for *E.coli* of nickel nitrate and nickel nanoparticles were recorded. *T.brevifolia* tree contains an anti-cancerous substance called Taxol. From leaves of the *T.brevifolia* tree, HPLC test was carried out and Taxol was registered. Anticancer activity of *T.brevifolia* leaves extract, nickel nitrate and nickel nanoparticle were investigated. Bio-synthesized NiNPs showed a cytotoxic effect on human Breast cancer cell line MCF-7. Finally, in the MTT test of *T.brevifolia* extract, nickel nitrate and nickel nanoparticle on Breast cancer cell line MCF-7 great anti-cancer effects were observed. Ni nanoparticles also exhibited more anticancer effect compared to the pure extracts. One of the nickel nanoparticles dilution that showed the best anti-cancer treatment was selected and TEM image was recorded. TEM micrograph suggests that the size of particles is 50 nm.

REFERENCES

1. F. Porta, L. Prati, M. Rossi, S. Coluccia, G. Martra, *Catal. Today.*, **61**, 165 (2000).
2. C. E. Hoppe, M. Lazzari, I. Pardinas-Blanco, M. A. Lopez-Quintela, *Langmuir*, **22**, 7027 (2006).
3. J. L. Lyon, D. A. Fleming, M. B. Stone, P. Schiffer, M. E. Williams, *Nano Lett.*, **4**, 719 (2004).
4. Y. Lu, Y. Mei, M. Schrinner, M. Ballauf, M. W. Moller, J. Breu, *J. Phys. Chem. C.*, **111**, 7676 (2007).
5. M. T. Swihart, *Colloid Interface.*, **8**, 127–133(2003).
6. S. Eustis, M. A. El-Sayed, *Chem. Soc. Rev.*, **35**, 209 (2006).
7. R. Joerger, T. Klaus, C. G. Granqvist, *Adv. Mater.*, **12**, 407 (2000).
8. A. Ingle, M. Rai, A. Gade, M. Bawaskar, *J. Nanoparticle Res.*, **11**, 2079 (2009).
9. H. J. Lee, G. Lee, N. R. Jang, J. M. Yun, J. Y. Song, B. S. Kim, *Nanotechnology.*, **1**, 371 (2011).
10. K. Govindaraju, S. Tamilselvan, V. Kiruthiga, G. Singaravelu, *J. Biopestic.*, **3**, 394 (2010).
11. A. Hamidi, and S. Jedari, *Sharif. Civ. Eng. J.* **29**, 29 (2011).
12. R. S. Babu, P. Prabhu, S. S. Narayanan, *Talanta.*, **110**, 135 (2013).
13. A. Salimi, A. Noorbakhash, E. Sharifi, A. Semnani, *Biosens. Bioelectron.*, **24**, 792 (2008).
14. A. S. Adekunle, K. I. Ozoemena, *J. Electroanal. Chem.*, **645**, 41 (2010).
15. T. Hyeon, *Chem. Comm.*, **9**, 927 (2003).
16. R. Karmhag, T. Tesfamichael, E. Wäckelgård, G. A. Niklasson, M. Nygren, *Solar Energ.*, **68**, 329 (2000).
17. A. A. Mariam, M. Kashif, S. Arokiyaraj, *Digest J. Nanomater. Biostructures.*, **9**, 1007 (2014).
18. F. Alonso, P. Riente, M. Yus, *Euro. J. Organic Chemis.*, **29**, 4908 (2008).
19. A. Dhakshina Moorthy, K. Pitchumani, *Tetrahedron Let.*, **49**, 1818 (2008).
20. F. Alonso, P. Riente, M. Yus, *Tetrahedron*, **64**, 1847 (2008).
21. F. Alonso, P. Riente, M. Yus, *Euro. J. Organic Chemis.*, **34**, 6034 (2009).
22. X. K. Li, W. J. Ji, J. Zhao, S. J. Wang, C. T. Au, *J. Catalysis.*, **236**, 181 (2005).
23. Y. Li, B. Zhang, X. Xie, J. Liu, Y. Xu, W. Shen, *J. Catalysis.*, **238**, 412 (2006).
24. C. J. Pandian, R. Palanivel, S. Dhanasekaran, *Chin J Chem Eng.*, **23**, 1307 (2015).
25. H. Mahabadipour, and H. Ghaebi, *Appl. Therm. Eng.* **50**, 771 (2013).
26. S. Hosseini, A. Shamekhi, and A. Yazdani, *J. Renew. Sust. Ener.* **4**, 043107 (2012).
27. M. Vaseem, N. Tripathy, G. Khang, Y. B. Hahn, *RSC Advances.*, **3**, 9698 (2013).
28. A. Y. Nobakht, R. K. Saray, A. Rahimi, *Fuel.* **90**, 1508 (2011).
29. J. N. Denis, A. E. Greene, D. Guenard, F. Gueritte Voegelein, L. Mangatal, P. Potier, *J Am Chem. Soc.*, **110**, 5917 (1988).
30. M. C. Wani, H. L. Taylor, M. E. Wall, P. Coggon, A. T. McPhail, *J Am Chem Soc.*, **93**, 2325 (1971).
31. R. Sathyavathi, M. B. Krishna, S. V. Rao, R. Saritha, D. N. Rao, *Adv Sci Lett.*, **3**, 138 (2010).
32. D. Inbakandan, C. Kumar, L. S. Abraham, R. Kirubakaran, R. Venkatesan, S. A. Khan, *Surf B.*, **111**, 636 (2013).
33. A. Sileikaite, I. Prosycevas, J. Puiso, A. Juraitis, A. Guobiene, *Mat. Sci. Medzia.*, **15**, 154 (2006).
34. M. M. Abdo, G. Elham, S. Nayereh, M. Y. Wan, S. Elias, *Polymers.*, **6**, 2435 (2014).
35. N. Khalid, O. Munetaka, D. Raquel, A. Mohammed, I. V. Kityk, B. Mosto, *J Alloys Compd.*, **509**, 5882 (2011).
36. C. Huimei, W. Jing, H. Dengpo, C. Xiaer, Z. Jiajia, S. Daohua, H. Jiale, L. Qingbiao, *Mater Lett.*, **122**, 166 (2014).
37. N. Kazem, S. Elias, R. Khadijeh, M. Y. Wan, *Radiat. Phys Chem.*, **79**, 1203 (2010).

38. A. Solomon, S. Mamuru Abubakar, B. Saminu, *Int J Appl Sci Biotechnol.*, **3**, 167 (2015).
39. C. J. Pandian, R. Palanivel, S. Dhanasekaran, *Chin J Chem Eng.*, **23**, 1307 (2015).
40. G. Angajala, A. Radhakrishnan, *Inflammation and Cell Signaling.*, **1**, 123 (2014).
41. I. Fatimah, *J. Adv. Res.*, **7**, 961 (2016).
42. A. Y. Nobakht, S. Shin, K. D. Kihm, D. C. Marable, and W. Lee, *Carbon*. **123**, 45 (2017).
43. J. Kurepa, R. Nakabayashi, T. Paunesku, M. Suzuki, K. Saito, E. G. Woloschak, A. J. Smalle, *Plant J.*, **77**, 443 (2014).
44. Q. Yun, J. Meng, S. Yuan, C. Lu, Z. Lin, Z. Xia, *Nanoscale Res Lett.*, **10**, 408 (2015).
45. J. P. Chitra, P. Rameshthangam, D. Solairaj, *Chin. J. Chem. Engin.*, **23**, 1307 (2015).
46. C. J. Pandian, R. Palanivel, S. Dhanasekaran, *J. Nanoparticles.*, **2016**, 1 (2016).
47. K. Mallikarjuna, G. Narasimha, G. Dillip, B. Praveen, B. Shreedhar, C. Sreelakshmi, B. Reddy, P. Deva, *J. Nanomater Biostruct.*, **6**, 181 (2011).
48. D. D. Evanoff, G. Chumanov, *Chem. Phys. Chem.*, **6**, 1221 (2005).
49. A. Y. Nobakht, Y. A. Gandomi, J. Wang, M. H. Bowman, D. C. Marable, B. E. Garrison, D. Kim, S. Shin, *Carbon*. **132**, 565 (2018).
50. K. Vasudeo, K. Pramod, *Biotechnol Ind J.*, **12**, 106 (2016).
51. C. J. Pandian, R. Palanivel, S. Dhanasekaran, *J Nanoparticles*, **2016**, 12 (2016).
52. A. Solomon, N. Mamuru Jaji, *J. Nanostructure Chemist.*, **5**, 347 (2015).
53. G. Elango, S.M. Roopan, K.I. Dhamodaran, K. Elumalai, N.A. Al Dhabhi, M.V. Arasu, *J. Photochemistry Photobiology, B: Biology.*, **162**, 162 (2016).
54. P. Rameshthangam, J. P. Chitra, *J. Mater. Sci. Technol.*, **25**, 89 (2017).
55. X. S. Wang, X. Liu, L. Wen, Y. Zhou, Z. Li, *Sep Sci Technol.*, **43**, 3712 (2008).